Microscopic evidence for scission neutrons

Ibrahim Abdurrahman[1,*], *Matthew* Kafker[2], *Aurel* Bulgac[2], and *Ionel* Stetcu[1]

[1]Theretical Division, Los Alamos National Laboratory, Los Alamos, NM 87545, USA
[2]Department of Physics, University of Washington, Seattle, WA 98195, USA

Abstract. We discuss the neck rupture stage of fission and the emission of particles afterwards, two extremely rapid and highly non-equilibrium processes. Currently, the neck rupture cannot be directly probed by experiment, highlighting the importance of reliable theoretical predictions for this stage of fission. Time-dependent density functional theory (TDDFT) is used to simulate the spontaneous fission of ^{252}Cf. In conjunction with statistical models, inputs from microscopic calculations can be used to make predictions for prompt neutron and gamma emission spectra, quantities which can be experimentally measured. Here we characterize the scission mechanism within TDDFT and estimate the number of scission neutrons and their kinetic energies.

1 Introduction

In 1939, Nuclear fission was discovered by Hahn and Strassmann [1], and its main mechanism elucidated by Meitner and Frisch [2]. In the same year, the idea of scission neutrons (SNs) was first proposed by Bohr and Wheeler [3]:

We consider briefly the third possibility that the neutrons in question are produced during the fission process itself. In this connection attention may be called to observations on the manner in which a fluid mass of unstable form divides into two smaller masses of greater stability; it is found that tiny droplets are generally formed in the space where the original enveloping surface was torn apart.

For a long time after, the idea remained dormant, until the 60s, when Bowman et al. [4] computed the angular distributions of neutrons emitted from the spontaneous fission of ^{252}Cf. They observed significant deviations from the emission expected if the isotropic hypothesis held true: all neutrons are expected to be emitted isotropically from post Coulomb accelerated FFs. They attributed this difference to SNs, by adding a "corrective" SN contribution, estimated by assuming all SNs are emitted isotropically from the center of the compound system at scission.

* e-mail: ia4021@lanl.gov

Beyond the 60s, there was no longer a consensus among the community as to whether or not scission neutrons existed. For models which did include them, predictions for their properties varied drastically. Experimental efforts to estimate the percentage of SNs varied from as low as 1% to as high as 15% [5-14]. In part this is due to the model dependence of such estimates, with the majority of the above studies assuming the same model for SNs as Bowman did in 1962.

2 Theoretical framework

To model fission, we use TDDFT, a generalized framework for treating low energy nuclear phenomena involving many interacting nucleons [15]. TDDFT explicitly treats the dynamics of pairing correlations and is formulated in terms of quasi-particle wavefunctions. In practice simulations involve evolving $4N_x\ N_y\ N_z$ quasi-particle wavefunctions, each comprising of $4N_x\ N_y\ N_z$ double complex elements for approximately 30,000 timesteps, where N_x, N_y, N_z represent the dimensions of the lattice. In order to allow emitted scission nucleons to spatially separate from the compound system we performed studies for the spontaneous fission of ^{252}Cf with lattices of size $N_x = 48$, $N_y = 48$, $N_z = 100$, which required the use of full machine runs on both Summit and Sierra. In principle, even larger lattices are required to more cleanly extract SN properties.

The quasi-particle wavefunctions are evolved via:

$$i\hbar\frac{\partial\psi_k(\boldsymbol{r},t)}{\partial t} = i\hbar\frac{\partial}{\partial t}\begin{pmatrix} u_{k\uparrow}(\boldsymbol{r},t) \\ u_{k\downarrow}(\boldsymbol{r},t) \\ v_{k\uparrow}(\boldsymbol{r},t) \\ v_{k\downarrow}(\boldsymbol{r},t) \end{pmatrix} =$$

$$\begin{pmatrix} h_{\uparrow\uparrow}(\boldsymbol{r},t)-\mu & h_{\downarrow\uparrow}(\boldsymbol{r},t) & 0 & \Delta(\boldsymbol{r},t) \\ h_{\downarrow\uparrow}(\boldsymbol{r},t) & h_{\downarrow\downarrow}(\boldsymbol{r},t)-\mu & -\Delta(\boldsymbol{r},t) & 0 \\ 0 & -\Delta^*(\boldsymbol{r},t) & -(h^*_{\uparrow\uparrow}(\boldsymbol{r},t)-\mu) & -h^*_{\downarrow\uparrow}(\boldsymbol{r},t) \\ \Delta^*(\boldsymbol{r},t) & h_{\uparrow\downarrow}(\boldsymbol{r},t) & -h^*_{\downarrow\uparrow}(\boldsymbol{r},t) & -(h^*_{\downarrow\downarrow}(\boldsymbol{r},t)-\mu) \end{pmatrix}\begin{pmatrix} u_{k\uparrow}(\boldsymbol{r},t) \\ u_{k\downarrow}(\boldsymbol{r},t) \\ v_{k\uparrow}(\boldsymbol{r},t) \\ v_{k\downarrow}(\boldsymbol{r},t) \end{pmatrix}, \quad (1)$$

where the quasi-particle Hamiltonian is defined via the minimization condition $\frac{\delta\mathcal{E}}{\delta\psi_k} = 0$, where $\mathcal{E}$, represents the nuclear energy density function (NEDF). We choose the SeaLL1 NEDF for this study, whose interaction term is given by:

$$\mathcal{E}_{\text{SeaLL1}} = \sum_{j=0}^{2}\left(a_j n_0^{\frac{5}{3}} + b_j n_0^{\frac{5}{3}} + c_j n_0^{\frac{5}{3}}\right)\left(\frac{n_1}{n_0}\right)^{2j}$$

$$+\sum_{t=0,1}\left(C_t^{n\Delta n} n_t \Delta n_t + C_t^{\nabla J}[n_t\boldsymbol{\nabla}\cdot\boldsymbol{J}_t + \boldsymbol{s}_t\cdot(\boldsymbol{\nabla}\times\boldsymbol{J}_t)]\right). \quad (2)$$

For more specifics see [15]. SeaLL1 was chosen, since it contains the smallest number of phenomenological parameters required to correctly describe nuclear matter (8), all of which are tied to specific nuclear properties: density and binding energy of nuclear matter (2 parameters), proton charge (1 parameter), nuclear surface tension (1 parameter), strength of pairing and spin orbit interactions (2 parameters), symmetry energy and its density dependence (2 parameters). It is reasonable to expect that if these few characteristics are

accurate, and if the theoretical framework is sound, one should obtain accurate predictions for a wide range of fission observables: masses, charge radii, spectra, and so forth, see [16-17].

3 Neck rupture

The integrated neck density, shown in Fig. 1, is defined as

$$n_{\mathrm{neck},\tau}(t) = \int dxdy\, n_{\mathrm{neck},\tau}(x, y, z_{\mathrm{neck}}, t),\ \tau = \mathrm{n}, \mathrm{p}, \tag{3}$$

where the z_{neck} represents the position on the fission axis within the compound nucleus where the number density obtains its smallest value. The neck decays slowly, until it reaches a critical diameter, after which it decays rapidly. In the lower panel of Fig. 1, different curves represent different trajectories, which correspond to various initial conditions around the saddle point. These conditions have approximately equal energy to the saddle point and are characterized by different quadrupole (Q_{20}) and octupole (Q_{30}) deformations. The time to reach scission can vary significantly depending on the initial conditions, but typically range from 1,000 to 3,000 fm/c.

These results illuminate several points, unknown until now,

1. First, the "wrinkle" in the nuclear density, where the nucleus ruptures is determined a long time before the nucleus reaches scission. The neck does not rupture randomly within TDDFT, and its position is determined by the quasiparticle energy spectrum and/or the shell structure around the saddle point.
2. Second, the proton neck finishes rupturing earlier than the neutron neck does, as shown in the lower panel in Fig. 1. As a result, the neck is mostly sustained by only neutrons moments before the full rupture. During this time interval, the number of neutrons per unit area at the neck is orders of magnitude greater than the number of protons per unit area at the neck. After the neck ruptures, the integrated neutron and proton densities at the neck quickly reach their equilibrium values.
3. Third, the rupture is unarguably the fastest stage of the fission dynamics, starting from the capture the incident neutron and formation of the compound nucleus, until all fission products have emitted. It decays significantly faster than the time it takes the fastest nucleon to communicate information between the two primordial FFs.
4. Fourth, the neck decay dynamics are universal, independent of the initial condition chosen (deformation or nuclear system, elaborated further upon in the caption of Fig. 1). Specifically, once the neck begins to rupture its decay rate is approximately the same across all trajectories, and the time for the full rupture to occur, which is approximately 200 fm/c, also does not vary much (see the lower panel of Fig. 1).
5. Last, the scission mechanism emerging from TDDFT of the fission dynamics is at odds with previous models, including the Brosa random rupture model [18], since it predicts that the neck rupture cannot occur at random points, but is rather remains fixed after the compound passes the saddle. Additionally, in order for the Brosa model to generate wide FF mass and charge yields, it requires unrealistically long neck, which dynamically do not form in TDDFT [18]. These results are also in contradiction with scission-point models [19], which assumes the system

reaches a static equilibrium at the scission point. The neck rupture is too rapid a process for this to be the case, as discussed above in point 3.

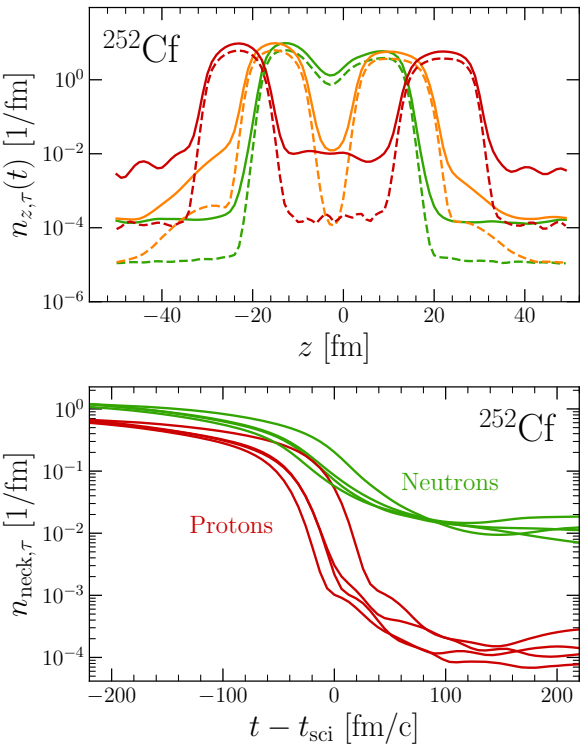

Fig. 1. The integrated nucleon density along the axis of fission, $nz,\tau\ (t) = \int dxdy\ n\tau\ (x, y, z, t)$, is shown in the upper panel for various times for the fission of ^{252}Cf. The green lines represent before scission, the orange lines towards the end of the neck rupture, and the red line long after scission. Neutrons are shown as solid lines and protons are shown as dashed lines. In the bottom panel, the neutron (green lines) and proton (red lines) number densities are integrated over the transverse coordinates (as described in equation 3). The various lines represent trajectories evolved from different initial conditions (deformed compound systems) beyond the outer saddle, with energies roughly equal (to within 1 MeV) to the ground state. For more specific details please see [16].

4 Scission neutrons

After the neck ruptures, a number of nucleons are emitted in the plane perpendicular to the fission axis (see Fig. 2). After a sufficient time, additional nucleons are emitted in front of the FFs. This so called "sling shot" mechanism was theoretically suggested earlier by Mädler in 1984 [20], who termed it the "catapult" mechanism. He conjectured the densities of the FFs near the neck would reabsorb into the FFs, after the rupture, and hence cause nucleons to travel through the bodies of the FFs and subsequently escape in front of them. In TDDFT simulations, the emitted nucleons emerge as three distinct clouds, one transverse ring perpendicular to the fission axis and two in front of the FFs. This universal signal has appeared across all trajectories and nuclear systems considered hence far.

The neutrons emitted are free, containing a kinetic energy per nucleon that is 3 times as large the final kinetic energy of the light FF (post Coulomb acceleration). Additionally, their interaction energy comprises less than 1% of their kinetic energy. For ^{252}Cf the average kinetic energy of a scission neutron is given by 2.67 ± 0.24 MeV, with an average of 0.55 ± 0.02 neutrons emitted at scission.

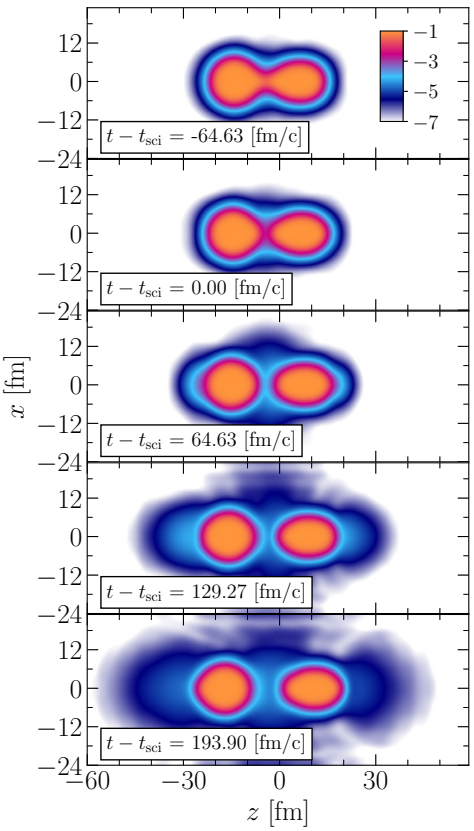

Fig. 2. Time series of the neutron number density in log scale for a typical fission trajectory.

5 Conclusion

Here, we presented a fully microscopic study of the neck rupture during fission dynamics and the emission of scission neutrons for the spontaneous fission of ^{252}Cf. We investigated the neck rupture, the fastest stage of fission, and the related emission of nucleons within the same period. Within TDDFT, the neck rupture is not random, but rather fixed once the compound system reaches the outer saddle point and remains stationary during the nucleus' descent to scission. Its dynamics are universal, holding across all currently studied trajectories. Similarly, the signal of scission neutrons is also universal, always appearing as three distinct clouds, with the transverse and longitudinal components (with respect to the fission axis), appearing in equal proportion. We have established that, on average, scission neutrons comprise of ~15% of total prompt neutrons emission per fission event, and that they carry a higher average kinetic energy. Aspects of the neck dynamics, and related emission of nucleons at the same stage, can act as theoretical inputs for semi-phenomenological fission models [21-23]. The existence of scission neutrons is a hotly debated topic over the years [24-48], since Bohr and Wheeler first proposed it in the same year as the discovery of fission

[3], and still lack direct experimental verification. Additionally, during scission, we also see a small fraction of charged particle emission. For extended results and discussion, including studies involving the fission of ^{236}U and ^{240}Pu, see [49].

We thank Kyle Godbey and Guillaume Scamps for many useful discussions. The work of I.A. and I.S. was supported by the U.S. Department of Energy through the Los Alamos National Laboratory. The Los Alamos National Laboratory is operated by Triad National Security, LLC, for the National Nuclear Security Administration of the U.S. Department of Energy Contract No. 89233218CNA000001. I.A. and I.S. gratefully acknowledges partial support and computational resources provided by the Advanced Simulation and Computing (ASC) Program. The work of M.K. and A.B. was supported by the US DOE, Office of Science, Grant No. DE-FG02-97ER41014 and also partially by NNSA cooperative Agreement DE-NA0003841, and is greatly appreciated. This research used resources of the Oak Ridge Leadership Computing Facility, which is a U.S. DOE Office of Science User Facility supported under Contract No. DE-AC05-00OR22725.

References

1. O. Hahn and F. Strassmann, Naturwissenschaften **27**, 11 (1939)
2. L. Meitner, L. and O. R. Frisch, Nature **143**, 239 (1939)
3. N. Bohr and J. A. Wheeler, Phys. Rev. **56**, 426-450 (1939)
4. H. R. Bowman, S. G. Thompson, J. C. D. Milton, and W. J. Swiatecki, Phys. Rev. **126**, 2120 (1962)
5. A. Gavron and Z. Fraenkel, Phys. Rev. C **9**, 632–645 (1974)
6. J. S. Pringle and F. D. Brooks, Phys. Rev. Lett. **35**, 1563 (1975)
7. C. B. Franklyn, C. Hofmeyer, and D. W. Mingay, Phys. Lett. B **78**, 564 (1978)
8. C. B. Franklyn, Radiation Effects **92**, 323 (1986)
9. C. Budtz-Jørgensen and H.-H. Knitter, Nuclear Physics A **490**, 307 (1988)
10. M. S. Samant, R. P. Anand, R. K. Choudhury, S. S. Kapoor, and D. M. Nadkarni, Phys. Rev. C **51**, 3127 (1995)
11. J. K. Hwang et al., Phys. Rev. C **60**, 044616 (1999)
12. Vorobyev, A.S., Shcherbakov, O.A., Gagarski, A.M., Val´ski, G.V., and Petrov, G.A., EPJ Web of Conferences **8**, 03004 (2010)
13. I. S. Guseva, A. M. Gagarski, V. E. Sokolov, G. A. Petrov, A. S. Vorobyev, G. V. Val'sky, and T. A. Zavarukhina, Phys. Atom. Nuclei **81**, 447 (2018)
14. A. S. Vorobyev, O. A. Shcherbakov, A. M. Gagarski, G. A. Petrov, G. V. Val'ski, and T. E. Kuz'mina, J. Exp. Theor. Phys. **127**, 659 (2018)
15. S. Jin K. J. Roche, I. Stetcu, I. Abdurrahman, and A. Bulgac, Comput. Phys. Comm. **269**, 108130 (2021)
16. A. Bulgac, S. Jin, K. J. Roche, N. Schunck, and I. Stetcu, Phys. Rev. C. **100**, 034615 (2019)
17. A. Bulgac, M. M. Forbes, S. Jin, R. N. Perez, and N. Schunck, Phys. Rev. C. **97**, 044313 (2018)
18. U. Brosa, S. Grossmann, and A. Müller, Physics Reports **197**, 167 (1990)
19. B. D. Wilkins, E. P. Steinberg, and R. R. Chasman, Phys. Rev. C **14**, 1832 (1976)
20. P. Mädler, Z. Physik A **321**, 343 (1985)
21. B. Becker, P. Talou, T. Kawano, Y. Danon, and I. Stetcu, Phys. Rev. C **87**, 014617 (2013)
22. R. Vogt, J. Randrup, J. Pruet, and W. Younes, Phys. Rev. C **80**, 044611 (2009)

23. O. Litaize, O. Serot, D. Regnier, S. Theveny, and S. Onde, Physics Procedia **31**, 51 (2012)
24. R. R. Wilson, Phys. Rev. **72**, 189 (1947)
25. S. Debenedetti, J. E. Francis, W. M. Preston, and T. W. Bonner, Phys. Rev. **74**, 1645 (1948)
26. V. S. Stavinsky, JETP (Soviet Physics) **9**, 437 (1959)
27. R. W. Fuller, Phys. Rev. **126**, 684 (1962)
28. H. R. Bowman, S. G. Thompson, J. C. D. Milton, and W. J. Swiatecki, Phys. Rev. **126**, 2120 (1962)
29. S. S. Kapoor, R. Ramanna, and P. N. Rama Rao, Phys. Rev. **131**, 283 (1963)
30. K. Skarsvåg and K. Bergheim, Nuclear Physics **45**, 72 (1963)
31. A. Gavron and Z. Fraenkel, Phys. Rev. C **9**, 632–645 (1974)
32. Y. Boneh and Z. Fraenkel, Phys. Rev. C **10**, 893 (1974)
33. J. S. Pringle and F. D. Brooks, Phys. Rev. Lett. **35**, 1563 (1975)
34. C. B. Franklyn, C. Hofmeyer, and D. W. Mingay, Phys. Lett. B **78**, 564 (1978)
35. C. B. Franklyn, Radiation Effects **92**, 323 (1986)
36. C. Budtz-Jørgensen and H.-H. Knitter, Nuclear Physics A **490**, 307 (1988)
37. B. Milek, R. Reif, and J. Revai, Phys. Rev. C **37**, 1077 (1988)
38. U. Brosa and H.-H. Knitter, Z. Physik A **343**, 39 (1992)
39. M. S. Samant, R. P. Anand, R. K. Choudhury, S. S. Kapoor, and D. M. Nadkarni, Phys. Rev. C **51**, 3127 (1995)
40. J. K. Hwang et al., Phys. Rev. C **60**, 044616 (1999)
41. N. Carjan, P. Talou, and O. Serot, Nuclear Physics A **792**, 102 (2007)
42. M. Rizea, V. Ledoux, M. V. Daele, G. V. Berghe, and N. Carjan, Comp. Phys. Comm. **179**, 466 (2008)
43. N. Carjan and M. Rizea, Phys. Rev. C. **82**, 014617 (2010)
44. N. Carjan and M. Rizea, Phys. Lett. B. **747**, 178 (2015)
45. R. Capote, N. Carjan, and S. Chiba, Phys. Rev. C **93**, 024609 (2016)
46. I. S. Guseva, A. M. Gagarski, V. E. Sokolov, G. A. Petrov, A. S. Vorobyev, G. V. Val'sky, and T. A. Zavarukhina, Phys. Atom. Nuclei **81**, 447 (2018)
47. A. S. Vorobyev, O. A. Shcherbakov, A. M. Gagarski, G. A. Petrov, G. V. Val'ski, and T. E. Kuz'mina, J. Exp. Theor. Phys. **127**, 659 (2018)
48. N. Carjan and M. Rizea, Phys. Rev. C. **99**, 034613 (2019)
49. I. Abdurrahman, M. Kafker, A. Bulgac, and I. Stetcu. arXiv preprint arXiv:2307.13132 (2023)